



Full Text View

[Volume 30, Issue 6 \(June 2000\)](#)

Journal of Physical Oceanography

Article: pp. 1137–1157 | [Abstract](#) | [PDF \(1.85M\)](#)

Cold-Core Anticyclonic Eddies South of the Bussol' Strait in the Northwestern Subarctic Pacific

Ichiro Yasuda

Department of Earth and Planetary Physics, University of Tokyo, Tokyo, Japan

Shin-Ichi Ito and Yugo Shimizu

Tohoku National Fisheries Research Institute, Miyagi, Japan

Kaoru Ichikawa

Kyushu University, Fukuoka, Japan

Ken-Ichi Ueda

Miyagi Fisheries Research and Exploitation Center, Miyagi, Japan

Takayuki Honma

Hokkaido Kushiro Fisheries Experimental Station, Hokkaido, Japan

Masashi Uchiyama

Chiba Fisheries Experimental Station, Chiba, Japan

Kentaro Watanabe

Fukushima Fisheries Experimental Station, Fukushima, Japan

Noriyuki Sunou

Ibaraki Fisheries Experimental Station, Ibaraki, Japan

Kazushi Tanaka

Iwate Fisheries Technology Center, Iwate, Japan

Koji Koizumi

Shizuoka Fisheries Experimental Station, Shizuoka, Japan

ABSTRACT

Summer hydrographic surveys from 1993 to 1997 in the area south of the Kuril Islands in the northwestern subarctic Pacific showed the existence of anticyclonic eddies south of the Bussol' Strait at almost the same location but with variable sizes and intensities depending on the year. Every eddy had a cold, low salinity and low potential vorticity core, suggesting a strong influence from the Okhotsk Sea water. Two formation processes and annual variations were found with satellite data analyses. One is the case where eddies are locally formed south of the Bussol' Strait and intensified from summer to fall with the supply of Okhotsk Sea water as observed in 1993. In the other case, Kuroshio warm-core rings that had translated northeastward are arrested near the Bussol' Strait and amplified with the supply of Okhotsk Sea water as seen from summer to autumn in 1995. In winter, eddies tend to move northeastward with decay. The 1992 eddy moved northeastward then northward in winter and was eventually absorbed into the East Kamchatka Current. Mechanisms of the northeastward movements and the formations of the Bussol' eddies were discussed. A pseudo- β effect due to deep northeastward currents along the Kuril-Kamchatka Trench could be responsible for the northeastward movement. Since the volume transport of the coastal Oyashio water along the southern Kuril Islands is constrained by the potential vorticity difference between the Okhotsk Sea and the western subarctic gyre (WSAG), eddies could be generated and intensified when a outflow rate from the Okhotsk Sea exceeds the critical transport. The observed annual variations of the eddy evolution might be explained by the critical transport variation associated with an annual change of the WSAG.

1. Introduction

Recent observations show active mesoscale eddies in the North Pacific western subarctic gyre (WSAG) south of the Kuril Islands and Hokkaido (Lobanov et al. 1991; Rogachev et al. 1992, 1993, 1996a,b,c; Lobanov and Bulatov 1993; Rogachev 1997; Kawasaki 1993; Kawasaki and Kono 1992; Talley and Nagata 1995; Yasuda 1997; Kono and Kawasaki 1997a,b). We will refer to these mesoscale eddies south of Kuril Islands as *Kuril eddies*. We can see one example of eddies in the satellite infrared image as shown in Fig. 1. A large (over 300 km in diameter) and cold-core eddy was located south of the Bussol' Strait, centered at around 45°N and 153°E, and was entraining a cold water near the Bussol' Strait, which is deepest in the Kuril straits, and through which the Okhotsk Sea water mainly outflows (e.g., Talley and Nagata 1995). Since eddies located south of the Bussol' Strait will be focused in the present study, we will call such eddies *Bussol' eddies* in particular. Since Bussol' eddies are one of the most energetic and main hydrographic features in the WSAG, detailed studies are necessary to understand the physics of the northwestern subarctic south of the Kuril Islands where the East Kamchatka Current and the outflow from the Okhotsk Sea mainly through the Bussol' Strait merge and form the Oyashio, which is a source water of North Pacific Intermediate Water (NPIW) (Yasuda 1997; Yasuda et al. 1996a).

As pointed out by Yasuda (1997), property changes of the Oyashio water are fairly large around the Bussol' eddies; hence mixing around eddies might affect the formation of the Oyashio water and thus the formation of NPIW source water. Since the WSAG is a feeding and fishing ground for several pelagic fish species, their migration route and thus fishing grounds are possibly influenced by Bussol' eddies (Yasuda and Watanabe 1994; Yasuda and Kitagawa 1996; Yasuda et al. 1996b; Rogachev et al. 1996a).

Anticyclonic Kuril eddies have been reported to move northeastward (Kitano 1975; Lobanov et al. 1991; Yasuda et al. 1992; Kawasaki 1993). The movement is in the opposite direction of the westward eddy propagation on the planetary β , and it has not been well understood (Yasuda et al. 1992). The origin of some anticyclonic eddies is believed to be Kuroshio warm-core rings (Lobanov et al. 1991; Kawasaki 1993). However, since a cold-core anticyclonic eddy was observed south of the Bussol' Strait by Lobanov and Bulatov (1993), Kuril eddies are clearly not only from Kuroshio warm-core rings but also comprise subarctic waters. Satellite image analyses indicated the frequent southward deflections of thermal fronts south

Table of Contents:

- [Introduction](#)
- [Data](#)
- [Hydrographic structures](#)
- [Evolution of Bussol'](#)
- [Discussion](#)
- [Summary](#)
- [REFERENCES](#)
- [APPENDIX](#)
- [TABLES](#)
- [FIGURES](#)

Options:

- [Create Reference](#)
- [Email this Article](#)
- [Add to MyArchive](#)
- [Search AMS Glossary](#)

Search CrossRef for:

- [Articles Citing This Article](#)

Search Google Scholar for:

- [Ichiro Yasuda](#)
- [Shin-Ichi Ito](#)
- [Yugo Shimizu](#)
- [Kaoru Ichikawa](#)
- [Ken-Ichi Ueda](#)
- [Takayuki Honma](#)
- [Masashi Uchiyama](#)
- [Kentaro Watanabe](#)
- [Noriyuki Sunou](#)
- [Kazushi Tanaka](#)
- [Koji Koizumi](#)

of the Bussol' Strait (Hurlbert et al. 1996), suggesting successive eddy generations or stationary eddies in the area. The eddy formation, modification, movement, and decay processes might be thus very complicated; we need further investigations on Kuril eddies.

In the present study, we will focus on the hydrographic structure and variability of Bussol' anticyclonic eddies observed in every summer of 1993–97. We will report on the hydrographic structures using CTD data from 1993 to 1997 and on the variability with TOPEX/Poseidon and *ERS-1/2* altimetry data and NOAA Advanced Very High Resolution Radiometer (AVHRR) infrared images.

2. Data

The data used in the present study are CTD, satellite altimetry (TOPEX/Poseidon and *ERS-1/2*) data and NOAA AVHRR infrared images. We used CTD data obtained from multiship joint surveys for Pacific saury research in the area east of the Kuril Islands, Hokkaido, and Honshu (37°–48°N, 141°–163°E), which were conducted in the period from mid-July to mid-August from 1993 to 1997 (see Yasuda et al. 1994, 1995, 1996b, 1997, and 1999 for the detailed description of hydrographic structures and data sources). For the Okhotsk Sea Kuril Basin, we used CTD data by R/V *Hokko Maru* of Hokkaido National Fisheries Research Institute, which was conducted in September 1991 (Kawasaki and Kono 1992).

CTD data were taken down to almost 1000 dbar. Raw CTD data were averaged to 1-dbar intervals and the salinities were calibrated with salinity measurements of water samples. The 1-dbar data was smoothed by the ten time operation of $(A_{i-1} + 2A_i + A_{i+1})/4$ (A_i represents a water property at i th depth). As a conservative property independent of salinity and temperature, we used potential vorticity, defined here as

$$Q = -\frac{f}{\rho} \frac{\partial \sigma_\theta}{\partial z}.$$

For the estimation of Q , the density gradient was calculated as a least mean square of 50-dbar data for each 1-dbar interval. For isopycnal properties in 26.7–26.8 σ_θ , properties in the density range were averaged.

To detect the variability of Bussol' eddies, we use pseudo-absolute sea-surface dynamic height data combined from satellite altimetry and historical hydrographic data. The altimetry data are from TOPEX/Poseidon (T/P) and *ERS-1/2* satellites during their tandem period from October 1992 to October 1997. See the appendix for details on the data source and the methods of data processing.

3. Hydrographic structures of Bussol' eddies

a. Surface dynamic height


In each year anticyclonic eddies were observed at almost the same location south of the Bussol' Strait around 152°E, 44°N, as shown in the surface dynamic height fields relative to 800 dbar in summer from 1993 to 1997 (Fig. 2). However, the sizes and intensities estimated from height anomalies were highly variable from year to year (Fig. 2 and Table 1). The 1993 eddy was medium sized (diameter $\Phi = 250$ km) and relatively strong. The dynamic height anomaly $\Delta h = 12$ cm, the maximum eddy velocity $V_{\max} = 30$ cm s⁻¹ relative to 1000 dbar, the 0–1000 dbar eddy volume transport $\text{Tr}_e = 9$ Sv ($\equiv 10^6$ m³ s⁻¹), depth of the $\sigma_\theta = 27.2$ is $D = 930$ m, and the volume of the eddy with the cold water temperature less than 3°C is 2.6×10^{13} m³. The 1994 eddy with northeastward elongated shape was smaller and weaker ($\Delta h = 6$ cm) than the 1993 eddy.



The 1995 eddy was remarkably large ($\Phi = 350$ km) but weaker ($\Delta h = 12$ cm, $V_{\max} = 10$ cm s⁻¹, and $\text{Tr}_e = 5$ Sv) than the 1993 eddy. The eddy extended from the Bussol' Strait to the Subarctic Front (42°N, 154°E). The 1996 eddy was separated into two eddies: the eddy near the Bussol' Strait (1996A) was small with medium intensities ($\Delta h = 14$ cm) and the offshore eddy (1996B) was medium in size and weak ($\Delta h = 6$ cm). In 1997, two weak anticyclonic eddies were observed centered at around (A: 45°N, 154°E) and (B: 44°N, 151°E). Both of the 1997 eddies were small to medium in size and weak.



The dynamic height fields from satellite altimetry data (Fig. 3) show anticyclonic eddies corresponding to the hydrographic data (Fig. 2). The height anomalies of the anticyclonic eddies Δh_{alt} mostly agree with Δh from the hydrographic observations. The height anomaly of the 1996 A eddy from the altimetry was much smaller than the one from the hydrographic data. This is probably because the resolution was not enough although the eddy location was close to the

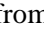
islands and the eddy diameter was small. The dynamic height fields also show general features; surface dynamic height is relatively high in the Okhotsk Sea, low in the WSAG, and high in the area south of the Subarctic Front. The WSAG is occupied with anticyclonic and cyclonic eddies. Anticyclonic eddies are remarkable in the Kuril Basin as shown in [Wakatsuchi and Martin \(1991\)](#) and [Yasuda \(1997\)](#). The dynamic height field averaged among the summer fields from 1993 to 1997 still shows an anticyclonic eddy south of Bussol' Strait, indicating that the Bussol' eddies were persistent in the summertime.

b. Vertical cross sections and water mass characteristics


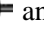
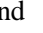

Every anticyclonic eddy observed south of Bussol' Strait had a cold ($T < 3^{\circ}\text{C}$) and fresh ($S < 33.5$ psu) core. Hence, cold-core anticyclonic eddies as reported by [Lobanov and Bulatov \(1993\)](#) are a common feature in the Bussol' eddies. For example, temperature, salinity, and potential density vertical sections across the 1993 Bussol' eddy are shown in [Fig. 4](#) . We can see a thick isopycnal layer in the density range of $26.6\text{--}27 \sigma_{\theta}$, that is, low potential vorticity characteristics of Okhotsk Sea mode water as shown in [Yasuda \(1997\)](#). This low potential vorticity core in the density range of $26.6\text{--}27 \sigma_{\theta}$ is a common feature in the Bussol' eddies observed in 1993–97, suggesting that the Bussol' eddies are strongly influenced by the Okhotsk Sea water mass.

The temperature and salinity in the cores of the eddy are variable from year to year although the cold, fresh, and low potential vorticity core is a common feature. In the 1993 eddy, cold ($T < 2^{\circ}\text{C}$) water occupied the core as shown in [Fig. 4](#) . In contrast, in the 1995 eddy ([Fig. 5](#) ) cold ($T < 2^{\circ}\text{C}$) water was observed only in a limited part on the southeastern side of the eddy. Warm ($T = 3^{\circ}\text{--}4^{\circ}\text{C}$) and saline ($S > 33.6$ psu) water was seen on the north western side of the core in the depth range of 100–200 m and in the density range of $26.6\text{--}26.7 \sigma_{\theta}$, although the low potential vorticity core was still observed in the density range of $26.7\text{--}27 \sigma_{\theta}$ as a common feature. This difference between the two eddies might be attributed to the formation and modification processes. The 1995 eddy is originated from a Kuroshio warm core ring that had a warm and salty core, as will be shown in the next section.

A diagram of potential temperature versus potential density ([Fig. 6a](#) ) shows that the Bussol' eddies had intermediate characteristics between the Okhotsk Sea water (OS in [Fig. 6](#) ) and the WSAG water (WSAG) in the density range of $26.9 < \sigma_{\theta} < 27.4$, suggesting that efficient mixing processes possibly occurred around the Bussol' Strait in this density range. The curve indicates that warm water of density $26.6\text{--}26.8 \sigma_{\theta}$ is the 1995 eddy, indicating the influence of subtropical waters.

As shown in [Yasuda \(1997\)](#), temperature and/or salinity are not very different around $26.8 \sigma_{\theta}$ between the Okhotsk and WSAG waters; potential vorticity is useful to identify the water-mass origin. Potential vorticity versus potential density profiles ([Fig. 6b](#) ) show that the Bussol' eddies were strongly influenced from the Okhotsk Sea water mass, which has vertical minimum potential vorticity at around $26.8 \sigma_{\theta}$. Every eddy had a vertical potential vorticity minimum in the density range $26.65\text{--}26.85 \sigma_{\theta}$, while the WSAG water has a vertical potential vorticity maximum around the density as shown in [Yasuda \(1997\)](#). The densities $\sigma_{\theta_{\min}}$ of the potential vorticity minimum Q_{\min} changed from year to year, while the core densities $\sigma_{\theta_{\min}}$ were in the range between 26.65 and $26.85 \sigma_{\theta}$. The Bussol' eddies observed in 1996 and 1997 were relatively weak with warmer, less dense $\sigma_{\theta_{\min}}$ and higher Q_{\min} cores compared with the eddies in 1993–95, although we need to note that the hydrographic measurements may not have been made in the center of the eddies, thereby biasing the results to larger Q_{\min} . These variations might be related to interannual variations in the Okhotsk Sea and WSAG (warmer and saltier shift of isopycnal water mass around $26.8 \sigma_{\theta}$ since 1995: Y. Kawasaki 1998, personal communication).

c. Potential vorticity along $26.7\text{--}26.8 \sigma_{\theta}$

[Figure 7](#)  shows the potential vorticity Q along the isopycnal layer of $26.7\text{--}26.8 \sigma_{\theta}$. [Yasuda \(1997\)](#) showed that the potential vorticity in this isopycnal layer can be used to identify the water mass origin. Low Q (< 15) Oyashio water is distributed near the Kuril Islands and is largely influenced from the Okhotsk Sea where the lowest potential vorticity exists in the North Pacific. High Q (> 30) water is WSAG water. Intermediate Q ($20 < Q < 30$) Oyashio water is distributed offshore of the low Q Oyashio water and with higher WSAG component. Comparison with the dynamic height maps ([Figs. 2](#)  and [3](#) ) and isopycnal salinity, temperature and acceleration potential maps (not shown) and [Fig. 7](#)  confirm the [Yasuda \(1997\)](#) conclusion that the isopycnal potential vorticity map is useful to identify the water mass origin.



In the Bussol' anticyclonic eddies, low Q (< 15) Oyashio water was commonly observed from 1993 to 1996. The 1997 eddy has somewhat higher $Q \sim 20$, but it is still low compared with the surrounding WSAG water. This indicates that the

Bussol' eddies are largely influenced from the water in the Okhotsk Sea in the density range as shown in the previous subsection.


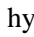
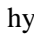
In the anticyclonic eddies located southeast of Hokkaido in 1993, 1994, and 1996, low- Q waters were also observed (see Figs. 2 and 7). This might be because the low Q water along the southern Kuril Islands and Hokkaido was entrained into the eddies through merging processes of like-signed vortices (e.g., [Yasuda 1995](#); [Yasuda and Flierl 1997](#); [Polvani 1988](#)).

4. Evolution of Bussol' eddies detected from satellite altimetry

a. Decay of the 1992 eddy

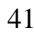
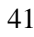
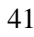
In autumn 1992, an intense anticyclonic Bussol' eddy was observed at around 46.5°N, 154°E (on 18 Oct 1992 in [Fig. 8](#)  for surface dynamic height and [Fig. 9](#)  for the eddy trajectory, time series of the height anomaly showing the eddy intensity and locations). This eddy translated northward in winter with decay in amplitude (average northward translation speed $C_y = 1.3 \text{ cm s}^{-1}$). Eventually, the eddy was absorbed into the East Kamchatka Current, moving southwestward (average eastward translation speed $C_x = -3.5 \text{ cm s}^{-1}$ and $C_y = -3.0 \text{ cm s}^{-1}$) and disappeared in February 1993. The origin and formation process of this intense anticyclonic eddy is not known; [Rogachev \(1997\)](#) reported this eddy had a cold, fresh, and low potential vorticity core and was located south of Bussol' Strait in the summer of 1992, suggesting that the eddy had been formed or amplified with the water supply from the Okhotsk Sea similarly to other Bussol' eddies.

b. Evolution of the 1993 eddy

In the period from January to May in 1993, a remarkable Bussol' eddy as seen in the fall of 1992 had not been observed. In July, an anticyclonic eddy started increasing amplitude near the Bussol' Strait ([Fig. 10](#) ). In early August when the hydrographic observations was performed, the eddy strength was not at the highest level ([Figs. 10](#)  and [11](#) ). The maximum amplitude was observed in November 1993. In the amplifying stage from July to November, the location of the eddy was almost stationary. With the fact that the core of the eddy was strongly influenced by the Okhotsk Sea water from the hydrographic observations described in the previous section, we can conclude that the 1993 eddy was formed locally near the Bussol' Strait and amplified with the supply of a cold, low salinity and low potential vorticity water from the Okhotsk Sea.

The 1993 eddy began moving northeastward in December 1993 with decay as observed in the 1992 eddy in the same winter season. The average translation speed $C_x = 2.0$ and $C_y = 2.0 \text{ cm s}^{-1}$ in the period from December 1993 to January 1994 when the eddy intensity was rapidly reduced. The decay process cannot be reliably obtained because the ERS high-resolution data was not available for the period from December 1993 to April 1994.

c. Evolution of the 1995 eddy

As mentioned in [section 3](#), the 1995 Bussol' eddy in summer 1995 was very large compared with other Bussol' eddies in summertime and contained warm and saline water. This eddy can be traced back to a Kuroshio warm-core ring at around 41.5°N, 146.5°E in the summer of 1994 ([Figs. 3](#) , [12](#) , and [13](#) ). This Kuroshio warm-core ring had a core temperature of 11°C and salinity of 34.4 psu in the summer of 1994. The eddy moved northeastward from August 1994 to June 1995 with decreasing amplitude. From August to December in 1994, the eddy moved northeastward relatively fast with translation speed $C_x = 3.2 \text{ cm s}^{-1}$ and $C_y = 2.1 \text{ cm s}^{-1}$ with slower decay than in the later period from January to June 1995. From January to June 1995, the eddy moved northeastward relatively slowly with translation speed $C_x = 0.5$ and $C_y = 0.9 \text{ cm s}^{-1}$ with more rapid decay.

From June to November 1995, the eddy remained at almost the same location south of Bussol' Strait and became amplified. These results indicated that the 1995 Bussol' eddy was originally a Kuroshio warm-core ring that moved northeastward and reached Bussol' Strait where the eddy was enhanced and modified with the supply of Okhotsk Sea water. This eddy began decaying and moving southwestward in December 1995 and disappeared until February 1996 near Bussol' Strait.

We conclude that the reason why the 1995 eddy was very large and contained warm and salty water is that it originated from the Kuroshio warm-core ring that was already intense and large and also enhanced with the supply of Okhotsk Sea water.

d. Annual changes of Bussol' eddies and the western subarctic gyre

Annual variations in surface dynamic topography from the satellite altimetry data are shown in Fig. 14, where 5-year averages were taken for each month. The 5-year average is not enough for climatological discussions, and strong signals in particular months and years affect the average field; however, we can derive some characteristic features of annual changes in Bussol' eddies and in the WSAG.

The southward deflection of dynamic height contours or the feature of isolated anticyclonic eddies, which correspond to Bussol' eddies, was observed even in the average fields in summer–autumn from August to December. The isolated eddy feature is clear from September to November; the eddy intensity generally increased from August to October and the maximum intensity is observed in November. In December, the eddy intensity was significantly reduced (not shown). This intensification of Bussol' eddies from summer to autumn and decay in winter agrees well with the evolution of individual eddies as shown in the previous subsections.

Annual variations in the intensity of the WSAG are evident. From winter to spring, the WSAG is enhanced; it is weakened from summer to autumn (Fig. 14). To show the variability in the intensity of the western boundary currents along the Kuril Islands (that is, the East Kamchatka Current), a time series of surface dynamic height differences in the areas of (47°–48°N, 152°–154°E) and (45°–48°N, 156°–158°E) is shown in Fig. 15. The former corresponds to the area near the Kuril Islands and the latter to the center of the WSAG. The annual change of the western boundary current is clear; it is most intense in spring and weakest in autumn. Similar results were also obtained by Isoguchi et al. (1997) with 1992–93 T/P data and by Kono and Kawasaki (1997b) using the direct current measurements south of Hokkaido.

The 12-month running mean sea-surface height difference (dots in Fig. 15) shows interannual variations of the East Kamchatka Current that weakened from 1993 to 1995 and strengthened from 1995 to 1997.

5. Discussion

a. Possible mechanism of northeastward movement of Kuril eddies

Both present and previous studies indicate that the movement of the Kuril anticyclonic eddies is northeastward except for the eddies near Bussol' Strait where they remained at almost the same location and became amplified from summer to fall. Kuroshio warm-core rings near the east coast of Honshu and Hokkaido Islands are also known to have a tendency to move northward or northeastward (Kitano 1975; Kuroda 1987; Yasuda et al. 1986; 1992). These poleward movements can be explained neither by the westward Rossby wave propagation due to planetary- β effect nor by the advection of the upper-layer mean flow whose direction is equatorward along the coasts of the Kuril, Hokkaido, and Honshu Islands. The self-propelling poleward movement of the anticyclonic eddies near the coast due to “mirror image effect” (Yasuda et al. 1986) might not be applicable to the northeastward moving Kuril eddies because distances between the eddies and the coasts are too large to be effective.

Recent deep flow measurements with mooring current meters and subsurface floats near Hokkaido and Honshu Islands reveal that deep mean flows below 1000 m are equatorward along bathymetric contours on the coastal side of the Kuril–Kamchatka Trench and poleward on the offshore side and around the deepest part (B. Owens and B. Warren 1996, personal communication; S. Riser 1996, personal communication). Reid (1997) also suggested the poleward deep western boundary current in the latter area from hydrographic data.

This poleward deep mean flow can excite northeastward Rossby waves, even in the southwestward upper-layer mean flow. To show this briefly, we use two-layer quasigeostrophic equations with spatially uniform upper-layer zonal mean flow U_1 and lower-layer zonal mean flow U_2 . If we assume that the thickness of the lower layer (H_2) is much larger than the one in the upper layer (H_1), $H_1 \ll H_2$, and the lower-layer eddy is much lower in amplitude than in the upper layer and linearize the equations, we obtain an eastward phase velocity for the upper-layer wave fields as

$$C_p = U_1 - \frac{\beta L_R^2 + (U_1 - U_2)}{1 + L_R^2(k^2 + l^2)}$$

$$= \frac{U_1 L_R^2(k^2 + l^2) + U_2 - \beta L_R^2}{1 + L_R^2(k^2 + l^2)},$$

where $L_R = (g'H_1)^{1/2}/f$ is an internal radius of deformation for the upper layer and k and l are zonal and meridional wavenumbers, respectively. With the long-wave approximation, the phase velocity of the upper-layer long Rossby wave

$$C_p = U_2 - \beta L_R^2$$

are in the direction of the deep mean flow when $U_2 > \beta L_R^2$ and are regardless of the upper-layer mean flow U_1 . The observed deep mean flow velocity is 3–10 cm s⁻¹ and $\beta L_R^2 \sim 1$ cm s⁻¹; the Rossby waves thus can propagate northeastward. This propagation is caused by the pycnocline slope due to the vertical velocity shear between the upper and lower layers against the planetary vorticity gradient and is often called pseudo- β effect (Morel 1995; Morel and McWilliams 1997). For smaller scales (larger wavenumbers) and the zero upper-layer mean flow $U_1 = 0$, the eddy propagation becomes slower. For smaller-scale eddies and the presence of U_1 , the eddy propagation increasingly approaches the upper-layer mean flow U_1 with wavenumbers.

This explanation could be applied to the poleward movements of Kuroshio warm-core rings near the east coast of Honshu because the poleward deep western boundary current is suggested along the Japan Trench east of Honshu, Japan (Reid 1997).

b. Possible mechanism for growth of Bussol' eddies

The Bussol' anticyclonic eddy observed from summer to fall 1993 was locally formed and amplified with the supply of Okhotsk Sea water through Bussol' Strait. The 1995 eddy, which was originally a Kuroshio warm-core ring and moved northeastward, remained near the Bussol' Strait and became amplified with the supply of Okhotsk Sea water from summer to fall. Anticyclonic eddies were observed in almost the same location south of Bussol' Strait in every summer of 1993–97. These results suggest that the Bussol' anticyclonic eddies are often generated and intensified from summer to fall south of Bussol' Strait with the supply of the Okhotsk Sea water; of course, we must recognize that the tendency is not statistically significant and we need further study with data having longer time series.

The mechanism for the growth of an anticyclonic eddy by the supply of low potential vorticity (PV) water outflowing from a strait is discussed by Kubokawa (1991) in which the theory assuming a potential vorticity front between two constant PV waters was applied to the gyre of the Tsugaru Warm Current outflow from the Japan Sea through Tsugaru Strait. In the case of the Okhotsk Sea outflow, the situation is similar to the Tsugaru gyre in that the Okhotsk Sea water has low potential vorticity and the WSAG water has high potential vorticity. The difference in depth of the 27.2 σ_θ surface between the Okhotsk Sea and the western subarctic gyre is fairly significant and about 350 m (Yasuda 1997). In the Kubokawa's theory, the low potential vorticity water flows along the adjacent coast in the direction in which we observe the coast on the right side in the Northern Hemisphere after geostrophic adjustment. The volume transport of the alongshore low potential vorticity water is limited because the depths of the two waters with constant potential vorticities are constrained. When an outflow rate exceeds the critical transport, the excess flow with low potential vorticity must merge into an eddy, resulting in forming and/or intensifying the anticyclonic gyre near the strait.

The Kubokawa theory used a quasigeostrophic reduced-gravity model. Here we slightly modify the model into a semigeostrophic multilayer model with mean flow in the second layer with the alongshore velocity of V_2 (Fig. 16a). Two types of waters in the upper layer have constant potential vorticities, $Q_c = f/H_c$ and $Q_o = f/H_o$, on the coastal and offshore sides of the PV front, respectively, where f is the Coriolis parameter and H_c and H_o are the upper-layer thickness in the Okhotsk Sea and in the WSAG, respectively, at which relative vorticities can be ignored. If we assume no change in the alongshore direction ($\partial/\partial y = 0$) and steady states, the upper-layer alongshore velocities are described by the thermal wind relation:

$$V_1 = \frac{g'}{f} \frac{\partial h}{\partial x} + V_2$$

with constant potential vorticities Q_i ($i = c, o$)

$$Q_i = \frac{f}{H_i} = \left(\frac{\partial V_1}{\partial x} + f \right) / h,$$

where h is the upper-layer thickness, V_1 the upper-layer alongshore velocity, and V_2 the alongshore velocity just below the upper layer. The alongshore volume transport Tr of the coastal low potential vorticity water, that distributed in the


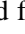
distance L from the coast, is



$$\text{Tr} = \int_0^L V_1 h \, dx = \frac{g'}{2f} [h^2|_{y=L} - h_c^2] + \int_0^L V_2 h \, dx,$$

where h_c is an upper-layer thickness at the coast. If we assume that a uniform lower-layer mean flow $\partial V_2 / \partial x = 0$, then the problem is analytically solved as

$$\begin{aligned} h &= H_c + (H_o - H_c) \cosh\left(\frac{x}{L_c}\right) \\ &\quad + b_0 \left[\cosh\left(\frac{x}{L_c}\right) - \frac{L_c}{L_o} \sinh\left(\frac{x}{L_c}\right) \right] \\ b_0 &= \frac{h_c - H_c - (H_o - H_c) \cosh\left(\frac{L}{L_c}\right)}{\cosh\left(\frac{L}{L_c}\right) + \frac{L_c}{L_o} \sinh\left(\frac{L}{L_c}\right)}, \end{aligned}$$

where $L_c = (g'H_c)^{1/2}/f$ and $L_o = (g'H_o)^{1/2}/f$ with the boundary conditions that $h = h_c$ at $x = 0$, $h = H_o$ at $x \rightarrow \infty$, and h and V_1 are continuous at $x = L$. If $H_o = 0$, we obtain simple the relation, $\text{Tr} = g'h^2_c/2f$. Thus, we can intuitively understand that the transport is limited by the thickness difference.

In the case of the second layer at rest ($V_2 = 0$), the maximum alongshore transport of the first term of the transport equation is about 4 Sv when $L = 30$ km for parameters corresponding to $27.2 \sigma_\theta$ as a density interface between the surface and the second layers ($f = 10^{-4} \text{ s}^{-1}$, $g' = 0.8 \times 10^{-2} \text{ m s}^{-2}$, $H_c = 750$ m, $H_o = 450$ m, and $h_c = 650$ m) adapting from the data of [Yasuda \(1997\)](#). When a transport out from the Okhotsk Sea is less than this critical value, the low PV water can flow away as a coastal boundary current ([Fig. 16b](#) ). Whereas, when the transport exceeds the critical value ([Fig. 16c](#) ), the low PV water must stay near the strait and forms an anticyclonic gyre because a large amplitude frontal disturbance propagates in the upstream direction and steady states could be kept in the downstream far enough from the strait as shown in [Kubokawa \(1991\)](#).

The annual variations of the tendency that the Bussol' anticyclonic eddies grow in the period from summer to fall might be explained by the annual variations of the western subarctic gyre. Annual variations of the WSAG were reported using satellite altimetry data as shown in the present study and [Isoguchi et al. \(1997\)](#) who found the Oyashio strong in winter–spring and weak in summer–autumn. [Kono and Kawasaki \(1997b\)](#) also showed annual variations of the Oyashio near the east coast of Hokkaido with direct current measurements and indicated that the velocity in the deeper part of the Oyashio is strong in the same direction as the surface Oyashio in winter–spring, while it is weak or stagnant in summer–autumn. This annual Oyashio change corresponds to the change of V_2 . In the period from winter to spring when the southwestward velocity V_2 of the Oyashio is stronger, a critical volume transport of low potential vorticity Okhotsk Sea water is increased because of the additional transport of $\int_0^L V_2 h \, dx$ ([Fig. 16b](#) ). When the Okhotsk Sea outflow transport is less than this critical transport, the gyre will stop growing and/or decay. The low PV water in the gyre could be transported as a coastal boundary current in the case where the gyre would become attached to the coastal boundary current as in the decay process of the 1995 eddy. Eddies could be isolated and move northeastward, decaying after the supply of Okhotsk Sea water is shut off as in the case of the 1992 eddy. From summer to fall when the WSAG is weakening (southwestward V_2 is decreasing), the Okhotsk Sea outflow transport exceeds the critical transport because the critical transport itself is decreasing ([Fig. 16c](#) ). The above explanation needs further investigation since both variations of the Okhotsk Sea outflow and WSAG have not been explained from direct measurements.

From Fig. 15, showing the annual variations in the East Kamchatka Current, the variation in annual sea-surface height change $\Delta\eta$ is up to 20 cm, suggesting annual surface velocity variations ΔU of roughly 20–40 cm s⁻¹ when we assume $\Delta U = g\Delta\eta/(f\Delta x)$ and a current width of 30–100 km. This annual velocity change could cause a 1–3-Sv change in the critical volume transport of the low PV water. The annual variation of the critical volume transport thus ranges from 4 to 7 Sv.

6. Summary

We have investigated cold and fresh core anticyclonic eddies south of Bussol' Strait (Bussol eddy) with data from 1993–97 summer hydrographic surveys and from satellite altimetry observations and discussed the evolution mechanism with simple theoretical models.

The hydrographic observations revealed the existence of cold, fresh, and less dense core anticyclonic eddies at almost the same location every summer, but with variable size and intensity. Water mass analyses showed that the eddies comprised mostly Okhotsk Sea water that has a potential vorticity minimum at around $26.8 \sigma_\theta$.

The altimetry observations revealed the annual variations of the Bussol' eddies. In early summer, anticyclonic eddies that were formed locally south of Bussol' Strait, or eddies that originated from Kuroshio warm-core rings and had moved northeastward, became enhanced. From summer to autumn, eddies remained south of the strait and became enlarged, modified with the supply of the low PV Okhotsk Sea water. The early developmental stage of the Bussol' eddies were thus observed in the summer hydrographic surveys when the size and intensity strongly depend on the evolution of each eddy. In contrast, from winter to spring, some eddies were isolated and moved northeastward, decayed, and eventually were absorbed into the East Kamchatka Current (EKC). Others decayed and disappeared near Bussol' Strait.

To understand these annual variations of the Bussol' anticyclonic eddies, we discussed the mechanism of eddy formation by the low PV Okhotsk Sea water through Bussol' Strait and the link to the annual variations of the western subarctic gyre circulation. In the upper layer shallower than the $27.2 \sigma_\theta$ density interface, a significant difference in thickness exists and, thus, PV between the Okhotsk Sea and the WSAG. The volume transport of the coastal boundary current with the low PV water (originating from the Okhotsk Sea) downstream far enough from Bussol' Strait is constrained by the thickness or PV difference and is also controlled by the alongshore velocity just below the density interface, the velocity which can be linked with the intensity of the WSAG circulation and thus the strength of the EKC. When the outflow rate from the Okhotsk Sea is less than a critical transport, the low PV water can be transported as a coastal boundary current without eddy formation near the strait (Fig. 16b). Whereas, when the outflow rate exceeds a critical value, the excess water must remain and forms an anticyclonic gyre near the strait (Fig. 16c).

From the above discussion, the annual variations in the Bussol' eddies could be attributed to the annual changes of WSAG, the outflow rate from the Okhotsk Sea, and the PV difference. In the present study, we focused on the annual variation of WSAG and hypothesized its link to the evolution of the eddies. From satellite altimetry data, the WSAG circulation and its western boundary current EKC are strong from winter to spring and weak from summer to fall, indicating higher critical transport in winter–spring and a lower one in summer–autumn. The estimate of the critical transport from simple models and observational data suggests that it ranges from 4 Sv in summer–autumn to 7 Sv in winter–spring. If we assume that the PV difference is almost constant and the outflow rate from the Okhotsk Sea to be relatively constant in the range of 4–7 Sv, the annual variations observed in the Bussol' eddies are consistent with the hypothesis that the WSAG annual variation controls the annual variation of the Bussol' eddies by changing the critical volume transport. We need the transport estimate of the outflow rate to validate this hypothesis.

The northeastward movement of eddies south of Kuril Islands and Kuroshio warm-core rings were confirmed from the satellite and hydrographic observations. The Bussol' eddy observed in summer 1995 was originally a Kuroshio warm-core ring near Hokkaido in summer 1994 that moved northeastward. A warm and saline remnant observed in the core of the 1995 eddy is a clear indication of the movement. From simple theoretical discussions, this northeastward movement could be due to the northeastward deep flow along the Kuril–Kamchatka Trench and pseudo- β effect that results from the slope of the density interface and, thus, potential vorticity gradient against the planetary β effect when there is a vertical velocity shear. The deep flow has recently been directly observed, validating the present hypothesis for the eddy propagation.

Acknowledgments

Discussions with Drs Kuniaki Okuda, Tokihiro Kono, Yasuhiro Kawasaki, Atsushi Kubokawa, V. B. Lobanov, and K. A. Rogachev were very valuable. The authors greatly appreciate the captains and the crew members of *Hokko-maru*, *Iwaki-maru*, *Shin-Miyagi maru*, *Chiba maru*, *Fuji maru*, *Iwate maru*, *Shin-Daitoh maru*, *Mito maru*, and *Hokushin maru* for preparing valuable data and participating joint observations. This work is partially supported by a grant in aid from the Ministry of Education, Science, and Culture and from the Science and Technology Agency of the Japanese government.

REFERENCES

- AVISO, 1996: *AVISO Handbook for Merged TOPEX/Poseidon Products*, AVI-NT-02-101-CN, Edition 3.0, AVISO, 21 pp..
- Emery, W. J., W. G. Lee, and L. Magaard, 1984: Geographic and seasonal distributions of Brunt–Väisälä frequency and Rossby radii in the North Pacific and North Atlantic. *J. Phys. Oceanogr.*, **14**, 294–317.. [Find this article online](#)
- Hurlbert, H. E., A. J. Wallcraft, W. J. Schmitz Jr., P. J. Hogan, and E. J. Metzger, 1996: Dynamics of the Kuroshio/Oyashio current system using eddy-resolving models of the North Pacific Ocean. *J. Geophys. Res.*, **101**, 941–976..
- Ichikawa, K., and S. Imawaki, 1994: Life history of a cyclonic ring detached from the Kuroshio Extension as seen by the Geosat altimeter. *J. Geophys. Res.*, **99** (C8), 15 953–15 966..
- , and —, 1996: Estimating the sea surface dynamic topography from Geosat altimetry data. *J. Oceanogr.*, **52**, 43–68..
- Isoguchi, O., H. Kawamura, and T. Kono, 1997: A study on wind-driven circulation in the subarctic North Pacific using the TOPEX/Poseidon altimeter data. *J. Geophys. Res.*, **102** (C1), 12 457–12 468..
- Kawasaki, Y., 1993: Modification and decay processes of a Kuroshio warm-core ring 86B in the northwestern subarctic Pacific (in Japanese). *Bull. Hokkaido Natl. Fish. Res. Inst.*, **56**, 43–54..
- , and T. Kono, 1992: Baroclinic water exchange in the Kuril Basin and the Northwestern Pacific in summer (in Japanese). *Umi to Sora*, **68**, 41–54..
- Kitano, K., 1975: Some properties of the warm eddies generated in the confluence zone of the Kuroshio and the Oyashio currents. *J. Phys. Oceanogr.*, **5**, 245–252.. [Find this article online](#)
- Kono, T., and Y. Kawasaki, 1997a: Modification of the western subarctic water by exchange with the Okhotsk Sea. *Deep-Sea Res.*, **44**, 689–711..
- , and —, 1997b: Results of CTD and mooring observations southeast of Hokkaido 1. Annual velocity and transport variations in the Oyashio. *Bull. Hokkaido Natl. Fish. Res. Inst.*, **61**, 65–81..
- Kubokawa, A., 1991: On the behavior of outflows with low potential vorticity from a sea strait. *Tellus*, **43A**, 168–176..
- Kuroda, R., 1987: Formations and movements of Kuroshio warm-core rings (in Japanese). *Kaiyo Mon.*, **19**, 265–274..
- Le Traon, P. Y., and F. Ogor, 1998: ERS-1/2 orbit improvement using TOPEX/Poseidon: The 2 cm challenge. *J. Geophys. Res.*, **103** (C4) 8045–8057..
- , P. Gaspar, F. Bouyssel, and H. Makhmara, 1995: Using TOPEX/Poseidon data to enhance ERS-1 data. *J. Atmos. Oceanic Technol.*, **12**, 161–170..
- Lobanov, V. B., and N. V. Bulatov, 1993: Physical structure and behavior of the Kuril eddies. *Proc. of Nemuro Workshop on Western Subarctic Circulation 1993*, PICES, 27-30..
- , K. A. Rogachev, N. V. Bulatov, A. F. Lomakin, and K. P. Tolmacher, 1991: Long-term evolution of the Kuroshio warm eddy. *Trans. Dokl. USSR Acad. Sci.*, **317**, 984–987..
- Morel, Y. G., 1995: The influence of an upper thermocline current on intrathermocline eddies. *J. Phys. Oceanogr.*, **25**, 3247–3252.. [Find this article online](#)
- , and J. McWilliams, 1997: Evolution of isolated interior vortices in the ocean. *J. Phys. Oceanogr.*, **27**, 727–748.. [Find this article online](#)
- Polvani, L. M., 1988: Geostrophic vortex dynamics. Ph.D. thesis, MIT/WHOI, WHOI-88-48, 221 pp..
- Reid, J. L., Jr., 1997: On the total geostrophic circulation of the Pacific ocean: Flow patters, tracers, and transports. *Progress in Oceanography*, Vol. 39, Pergamon, 263–352..
- Rogachev, K. A., 1997: Recent speeding up of the Pacific subarctic circulation. *WOCE Newslett.*, **26**, 40–42..
- , E. Carmack, M. Miyake, R. Thomson, and G. Yurasov, 1992: Drifting buoy in Oyashio anticyclonic ring (in Russian). *Dokl. Akad. Nauk*, **326**, 547–550..

- G. I. Yurasov, M. Miyake, and V. Sosnin, 1993: Structure of anticyclonic rings and volume transport of the Oyashio and Kamchatka Current in autumn 1990. *Proc. of Nemuro Workshop on Western Subarctic Circulation 1993*, PICES, 94–96..
- A. S. Salomatin, and E. C. Carmack, 1996a: Concentration of pelagic organisms at mesoscale fronts in the western subarctic Pacific: Small fish on long waves. *Fish. Oceanogr.*, **5**, 153–162..
- V. I. Yusupov, and E. C. Carmack, 1996b: On the internal structure of the Kuril Current anticyclonic rings (in Russian). *Oceanology*, **36**, 347–354..
- P. Y. Tishchenko, G. Y. Pavlova, A. S. Bychkov, E. C. Carmack, C. S. Wong, and G. I. Yurasov, 1996c: The influence of fresh-core rings on chemical concentrations (CO₂, PO₄, O₂, alkalinity, and pH) in the western subarctic Pacific Ocean. *J. Geophys. Res.*, **101** (C1), 999–1010..
- Talley, L. D., and Y. Nagata, Eds., 1995: The Okhotsk Sea and the Oyashio region. PICES Scientific Rep. 2, 227 pp..
- Teague, W. J., M. J. Carron, and P. J. Hogan, 1990: A comparison between the generalized digital environmental model and Levitus climatologies. *J. Geophys. Res.*, **95** (C5), 7167–7183..
- Wakatsuchi, M., and S. Martin, 1991: Water circulation of the Kuril Basin of the Okhotsk Sea and its relation to eddy formation. *J. Oceanogr. Soc. Japan*, **47**, 152–168..
- Yasuda, I., 1995: Geostrophic vortex merger and streamer development in the ocean with special reference to the merger of Kuroshio warm core rings. *J. Phys. Oceanogr.*, **25**, 979–996.. [Find this article online](#)
- 1997: The origin of the North Pacific Intermediate Water. *J. Geophys. Res.*, **102** (C1), 893–909..
- and Y. Watanabe, 1994: On the relationship between the Oyashio front and saury fishing grounds in the north-western Pacific. *Fish. Oceanogr.*, **3**, 172–181..
- and D. Kitagawa, 1996: Locations of early fishing grounds of saury in the Northwestern Pacific. *Fish. Oceanogr.*, **5**, 63–69..
- and G. R. Flierl, 1997: Two-dimensional asymmetric vortex merger: Merger dynamics and critical merger distance. *Dyn. Atmos. Oceans*, **26**, 159–181..
- K. Okuda, and K. Mizuno, 1986: Numerical study on the vortices near boundaries: Considerations on warm-core rings in the vicinity of east coast of Japan. *Bull. Tohoku Reg. Fish. Res. Lab.*, **48**, 67–86..
- and M. Hirai, 1992: Evolution of a Kuroshio warm-core ring: variability of the hydrographic structure. *Deep-Sea Res.*, **39** (Suppl.), S131–S161..
- T. Honma, S. Takasugi, Y. Izumi, T. Sato, R. Ando, K. Hiramoto, and Y. Katsumata, 1994: Hydrographic structure and saury fishing grounds from the western subarctic region to the Mixed Water Region in summer 1993. *Annual Report of the Research Meeting on Saury Resources* (issued by Tohoku National Fisheries Research Institute), **43**, 216–237..
- Y. Izumi, M. Uchiyama, K. Watanabe, K. Mori, T. Honma, T. Suno, K. Nozawa, and Y. Shimizu, 1995: Hydrographic structure in the western subarctic region in summer 1994 (in Japanese). *Annual Report of the Research Meeting on Saury Resources* (issued by Tohoku National Fisheries Research Institute), **44**, 266–289..
- K. Okuda, and Y. Shimizu, 1996a: Distribution and modification of North Pacific Intermediate Water in the Kuroshio–Oyashio interfrontal zone. *J. Phys. Oceanogr.*, **26**, 448–465.. [Find this article online](#)
- Y. Shimizu, K. Ueda, T. Honma, K. Watanabe, K. Mori, T. Suno, K. Tanaka, and M. Uchiyama, 1996b: Hydrographic structure in the western subarctic region and saury fishing grounds in summer 1995. *Annual Report of the Research Meeting on Saury Resources* (issued by Tohoku National Fisheries Research Institute), **45**, 234–255..
- and Coauthors, 1997: Hydrographic structure of the western subarctic region in summer 1996. *Annual Report of the Research Meeting on Saury Resources* (issued by Tohoku National Fisheries Research Institute), **46**, 240–256..
- and Coauthors, 1999: Hydrographic structure in the western subarctic region in summer 1997. *Annual Report of the Research Meeting on Saury Resources* (issued by Tohoku National Fisheries Research Institute), **47**, 248–259..
- Yi, Y., 1995: Determination of gridded mean sea surface from TOPEX, ERS-1 and GEOSAT altimeter data, Rep. 434, Dept. Geod. Sci. Surv., The Ohio State University, Columbus, OH, 93 pp..

7. Altimetry Data and Processing

All altimetry data are provided from AVISO as Corrected Sea Surface Heights (CORSSH) dataset. The CORSSH products are supplied by the CLS Space Oceanography Division, Toulouse, France (AVISO/Altimetry 1996; [Le Traon et al. 1995](#); [Le Traon and Ogor 1998](#)); the ERS products were generated as part of the proposal “Joint analysis of *ERS-1*, *ERS-2*, and TOPEX/Poseidon altimeter data for oceanic circulation studies,” selected in response to the Announcement of Opportunity for *ERS-1/2* by the European Space Agency (Proposal code:A02.F105). In the dataset, ordinary height corrections such as ionospheric, tropospheric, and tidal ones have been applied to the altimetry data, and *ERS-1/2* satellite orbit error is also removed by referring to accurate T/P satellite orbits.

The period of *ERS-1* altimetry data used in the present paper consists of three repeat-orbit periods. During the first (Phase C; from 6 October 1992 to 23 December 1993) and the third (Phase G; from 24 March 1995 to 2 June 1996) periods, *ERS-1* took 35-day exact repeating cycles with relatively high spatial resolution of about 75 km at midlatitude. Observations of *ERS-2*, which were started 29 April 1995, follow the same 35-day cycles as *ERS-1*. While in the second repeat-orbit period of *ERS-1* (Phase E and F; from 10 April 1994 to 21 March 1995), the satellite took two 168-day repeat cycles with 8-km shifted tracks, providing a very high spatial resolution but a low temporal resolution. Meanwhile, T/P provides observations with higher temporal resolution, 9.92 days, but with rougher spatial resolution, or about 300 km at midlatitude. In order to obtain sea surface dynamic topography with high resolutions in both time and space, we applied a multisatellite optimal interpolation to those data.

Sea surface height anomaly from the mean sea surface ([Yi 1995](#)) is optimally interpolated onto a 0.25° grid. The optimal interpolation method is basically similar to [Ichikawa and Imawaki \(1996\)](#), but we modified signal and error covariance functions as follows.

We set a signal covariance W as

$$W(\Delta x, \Delta y, \Delta t; x, y) = w_0(x, y)^2 \exp\left(-\frac{\Delta x^2}{L_x(y)^2} - \frac{\Delta y^2}{L_y(y)^2} - \frac{\Delta t^2}{L_t^2}\right),$$

where $w_0(x, y)$ stands for the magnitude of the signal variance at a point (x, y) ; L_x , L_y , and L_t for zonal, meridional, and temporal decorrelation scales; and Δx , Δy and Δt for differences in longitude, latitude, and time, respectively. The value of w_0 at each point is determined from 10-day lagged T/P covariance, and we empirically choose $L_x(y) = 100 \times \cos(y)$ km, $L_y(y) = 136.5 \times \cos(y)$ km, and $L_t = 15$ days.

For an error covariance ψ , two terms are to be considered; namely,

$$\psi(t_i, t_j, \mathbf{r}_{i,j}; x, y) = \sigma_0^2 \delta(t_i, t_j) + \sigma_1(x, y)^2 \exp\left(-\frac{\mathbf{r}_{i,j}^2}{l_r^2} - \frac{(t_i - t_j)^4}{l_t^4}\right),$$

where t_i and t_j represent times of two observations, $\mathbf{r}_{i,j}$ the distance between two observations, δ is Dirac's delta function, l_t is a decorrelation scale in time, and l_r that in space. The first term comes from measurement noise of each altimeters; the latter term also includes errors in height corrections such as tides. Subtracting the signal covariance $w_0(x, y)$ from the autocovariance of all altimetry observations, we determine $\sigma_1(x, y)$ at each point. From these autocovariances of each altimeters, we estimated σ_0 as 3.0 cm for TOPEX altimeter, 5.2 cm for Poseidon, 5.7 cm for *ERS-1* Phase C, 6.4 cm for other *ERS-1* phases, and 5.7 cm for *ERS-2*. Since we found $\sigma_1(x, y)$ generally smaller than $w_0(x, y)$ in the study area, the estimated results are less sensitive to the parameters l_t and l_r ; we set these parameters somewhat arbitrarily. Short-term sea surface variations are expected to have at least those temporal and spatial scales, therefore we choose 0.5 day for l_t as the semidiurnal tidal cycle, and the internal Rossby radius for l_r as a characteristic spatial scale for geostrophy; the latter is

calculated here by $25/[0.05 + \sin(y)]$ km to simulate observed values (Emery et al. 1984). Note that those parameters are kept the same for a period from 24 December 1993 to 9 April 1994 when no ERS altimeters are available; this results in that the estimated sea surface height anomaly in some areas would be unreliable since single T/P data cannot satisfy the required spatial resolution L_r .

The estimated sea surface height anomaly is further combined with 0.5° resolution climatological mean dynamic topography (Teague et al. 1990) to produce the composite sea surface dynamic topography, or approximated absolute dynamic topography (Ichikawa and Imawaki 1994).

Tables

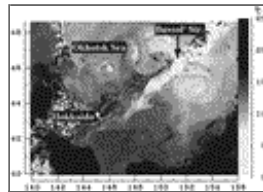
Table 1. Various parameters showing the characteristics of Bussol' eddies from summer hydrographic surveys during 1993–97.

Year	ϕ^*	λ^{**}	V_{max}^{\dagger}	V_{eddy}^{\ddagger}	D^{\S}	$\Delta\sigma^{\parallel}$	$\Delta h_{eddy}^{\#}$	$Q_{eddy}^{\&}$	σ_{θ}^{ζ}
1993	250	2.6	30	9	930	12	10	2	26.75
1994	200	1.7	20	4	630	6	6	2	26.8
1995	200	2.8	10	2	780	12	14	5	26.8
1996A	100	0.4	20	6	640	14	6	5	26.65
1996B	200	0.9	13	2	500	6	6	11	26.65
1997A	200	0.7	19	3	500	3	4	22	26.65
1997B	100	0.5	5	1	500	2	—	18	26.75

^{*} The eddy diameter d (km) is defined as twice the radius, which is the distance between the eddy center and the location at the maximum velocity.
[†] The volume V_{ed} (10^{10} m³) is defined as the dichothermal water with the temperature less than 2°C.
[‡] V_{max} (cm s⁻¹) is the eddy maximum geostrophic velocity relative to 1000 dbar.
[§] V_{eddy} (10^3 m² s⁻¹) is the eddy volume transport in 10^{10} dbar calculated from the geostrophic velocities relative to 1000 dbar.
[¶] D (m) is the maximum depth of the isopycnal contour of 27.2 σ_{θ} .
[#] $\Delta\sigma$ (cm) is the surface dynamic height anomaly estimated from hydrographic data relative to 800 dbar.
[&] Δh_{eddy} (cm) is the surface dynamic height anomaly from satellite altimeter.
^ζ σ_{θ} (10^{-3} m⁻³) is the potential vorticity at the vertical potential vorticity minimum.
^η σ_{θ} (10^{-3} m⁻³) is the density 1000 at the vertical potential vorticity minimum.

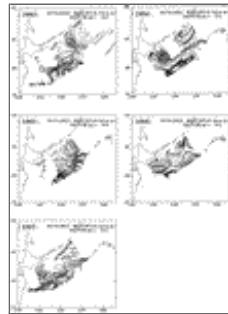
[Click on thumbnail for full-sized image.](#)

Figures



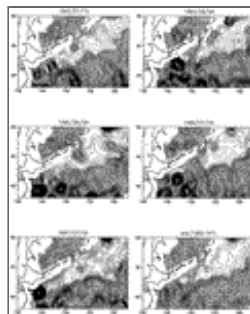
[Click on thumbnail for full-sized image.](#)

Fig. 1. NOAA AVHRR infrared image showing a large, cold-core anticyclonic eddy south of the Bussol' Strait on 10 October 1995.



[Click on thumbnail for full-sized image.](#)

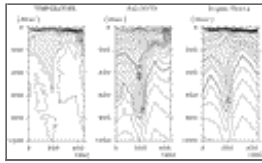
Fig. 2. Surface dynamic height referred to 800 dbar in July–August from 1993 to 1997. Contour intervals are 2 dyn cm.



[Click on thumbnail for full-sized image.](#)

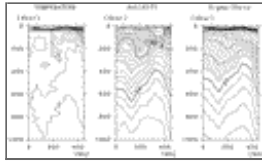
Fig. 3. Surface dynamic height from satellite altimetry data in July–August from 1993 to 1997, corresponding to [Fig. 2](#).

Contour intervals are 2 cm, and the areas of SSDH (sea surface dynamic height) >1.16 m are shaded.



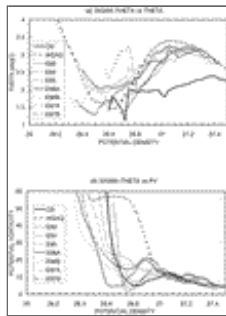
Click on thumbnail for full-sized image.

Fig. 4. Potential temperature, salinity, and potential density (σ_θ) vertical cross sections across the 1993 Bussol' eddy. The section location was denoted by large dots in Fig. 2. Left side is near the Bussol' Strait and the right is offshore. Contour intervals are 1°C, 0.1 psu, and 0.1 σ_θ . $T < 2^\circ\text{C}$, $33 < S < 33.6$ psu, and $26.5 < \sigma_\theta < 26.9$ are shaded.



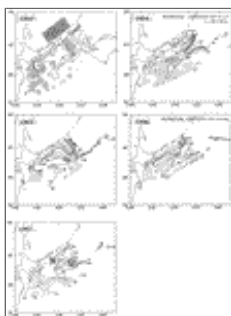
Click on thumbnail for full-sized image.

Fig. 5. Same as Fig. 4 but for the 1995 Bussol' large anticyclonic eddy.



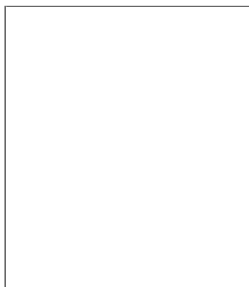
Click on thumbnail for full-sized image.

Fig. 6. (a) Potential temperature vs σ_θ profiles showing the characteristics of the core waters in the Bussol' eddies from 1993 to 1997. For references, the Okhotsk Sea water ('OS': thick solid curve) and the WSAG water ('WSAG': thick broken curve) are shown. (b) Same as (a) but for potential vorticity versus σ_θ profiles.



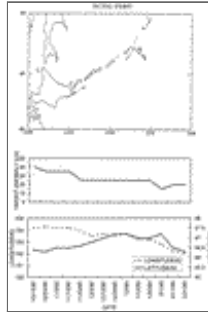
Click on thumbnail for full-sized image.

Fig. 7. Isopycnal potential vorticity distribution, defined as $Q = -f^{-1}\rho(\partial\rho/\partial z)$ ($10^{-11} \text{ m}^{-1} \text{ s}^{-1}$), along 26.7–26.8 σ_θ in July–August from 1993 to 1997. Contour interval is $10 \times 10^{-11} \text{ m}^{-1} \text{ s}^{-1}$. Shaded regions denote low Q water with $Q < 15$.



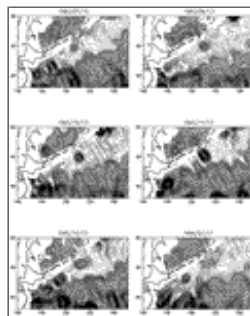
[Click on thumbnail for full-sized image.](#)

Fig. 8. Surface dynamic height from satellite altimetry to show the decay process of the 1992 eddy from October 1992 to March 1993. Contour intervals are 2 cm, and the areas of SSDH > 1.16 m are shaded.



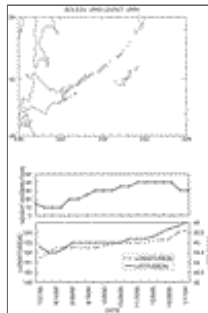
[Click on thumbnail for full-sized image.](#)

Fig. 9. (a) Trajectory, (b) surface dynamic height anomaly, and (c) longitude and latitude of the center of the 1992 Bussol' eddy; 10-day interval data were used.



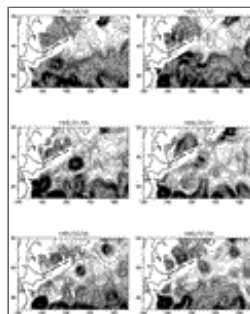
[Click on thumbnail for full-sized image.](#)

Fig. 10. Surface dynamic height from satellite altimetry to show the generation, amplification, and decay processes of the 1993 eddy from July 1993 to January 1994. Contour intervals are 2 cm, and the areas of SSDH > 1.1 m from December to July and SSDH > 1.16 m from August to October are shaded.



[Click on thumbnail for full-sized image.](#)

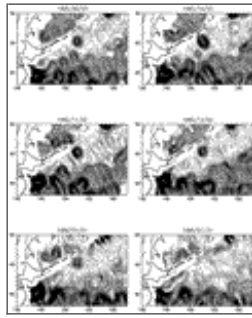
Fig. 11. (a) Trajectory, (b) surface dynamic height anomaly, and (c) longitude and latitude of the center of the 1993 Bussol' eddy; 10-day interval data were used.



[Click on thumbnail for full-sized image.](#)

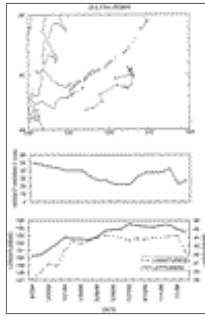
Fig. 12. Surface dynamic height from satellite altimetry to show the northeastward movement of a Kuroshio warm-core ring, amplification south of the Bussol' Strait, and decay processes of the 1995 eddy from September 1994 to January 1996. Contour

intervals are 2 cm,



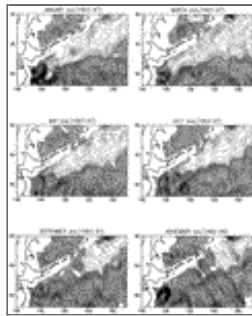
[Click on thumbnail for full-sized image.](#)

Fig. 12 (*Continued*) and the areas of SSDH > 1.1 m are shaded.



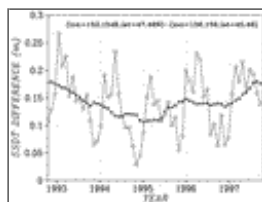
[Click on thumbnail for full-sized image.](#)

Fig. 13. (a) Trajectory, (b) surface dynamic height anomaly, and (c) longitude and latitude of the center of the 1995 Bussol' eddy; 30-day interval data were used.



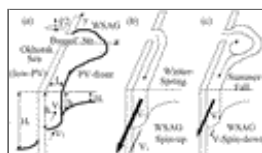
[Click on thumbnail for full-sized image.](#)

Fig. 14. Five-year average monthly surface dynamic height fields. Contour intervals are 2 cm, and the areas of SSDH > 1.1 m are shaded.



[Click on thumbnail for full-sized image.](#)

Fig. 15. Temporal variation in sea surface height difference between in the areas (47°–48°N, 152°–154°E) and (45°–48°N, 156°–158°E) to show the variability of the East Kamchatka Current from altimetry data. Dots represent the 5-year running mean.



[Click on thumbnail for full-sized image.](#)

Fig. 16. Schematic diagrams showing a model configuration (a), a coastal mode of the boundary current when the transport of

coastal low PV water is less than a critical value, (b) and a gyre mode when the transport exceeds the critical one (c).

Corresponding author address: Dr. Ichiro Yasuda, Department of Earth and Planetary Physics, Graduate School of Science, University of Tokyo, 7-3-1 Hongo, Bunkyo-ku, Tokyo 113-0033, Japan.

E-mail: ichiro@geoph.s.u-tokyo.ac.jp

[top](#) ▲



© 2008 American Meteorological Society [Privacy Policy and Disclaimer](#)

Headquarters: 45 Beacon Street Boston, MA 02108-3693

DC Office: 1120 G Street, NW, Suite 800 Washington DC, 20005-3826

amsinfo@ametsoc.org Phone: 617-227-2425 Fax: 617-742-8718

[Allen Press, Inc.](#) assists in the online publication of *AMS* journals.